

LETTERS

Charge Disproportionation in YNiO₃ Perovskite: An ab Initio Calculation

Xiaoguang Xu,[†] Xing Meng,[†] Chunzhong Wang,[†] Feng Wu,[‡] and Gang Chen^{*,†}

College of Materials Science and Engineering, Jilin University, Changchun, 130023, P. R. China, and
Beijing Institute of Technology, Beijing 100081, P. R. China

Received: July 17, 2003; In Final Form: December 5, 2003

The electronic structure of YNiO₃ is studied theoretically via ab initio calculation based on density functional theory. Band structures for monoclinic and orthorhombic phase are calculated. Calculation shows a band structure with insulating and metallic characteristics for monoclinic and orthorhombic phases, respectively. It was found that there are two different Ni ions, Ni(I) and Ni(II), with charges Ni^{(3-δ)+} and Ni^{(3+δ)+} in the monoclinic phase (*P*₂₁/*n*). The value of δ is calculated to be 0.24 from the intensity of Ni-3d nonbonding t_{2g} band on the basis of the density of states.

Efforts have been made to focus on the RNiO₃ perovskites (R = rare earth) for their attractive thermally driven metal–insulator (MI) transitions.^{1–11} It is suggested that the closing of the Ni–O–Ni angle (θ) by thermal contraction when the temperature decreases reduces the 3d–2p–3d orbital overlap beyond its critical value, producing a gap opening.^{2,3} It is also proposed that the rare earth nickelates are at the boundary between low-Δ metals and charge-transfer insulators, where Δ is the charge-transfer energy. If the volume expansion induced by the Ni–O bond occurs, the compound (such as Pr, Nd, or Sm nickelate) becomes an insulator.³ Among all the RNiO₃ perovskites, YNiO₃ is the most difficult to synthesize and was at first prepared by Demazeau et al. in 1971.¹⁰ Alonso et al. fully characterized it in 1999.^{11,12} The crystallography parameters are obtained on the basis of synchrotron X-ray diffraction (SXRD) and neutron powder diffraction (NPD).^{11,12} The results show that the Ni in YNiO₃ is in the trivalent state in the orthorhombic phase (space group *Pbnm*) at high temperature, and in a charge disproportionation state in the monoclinic phase (space group *P*₂₁/*n*) at low temperature, where the structure contains two crystallographically independent Ni positions,

which we will call Ni(I) and Ni(II) hereafter, which is confirmed by Mössbauer study.¹³ Both the very distinct isomer shift and the difference of the quadrupole splitting for the two types of ions support the viewpoint of the existence of two different NiO₆ octahedra.

Following Brown's bond valence model,¹⁴ δ was evaluated to be 0.33 for Ni^{(3-δ)+} and Ni^{(3+δ)+}.¹⁵ To study the characteristics of δ and the mechanism of the M–I transition clearly, we investigated the electronic structure of YNiO₃ theoretically with first principles.

Ab initio calculations were performed by the CASTEP¹⁶ software package based on the density functional theory (DFT) in the local density approximation (LDA) through the Cerius² graphical user interface. The electron–ion interaction is described by using ultrasoft pseudopotential. The cutoff energy is chosen as 380 eV, including a sufficient number of wave functions to obtain precise information about the electronic structure of the crystals. Calculations based on the crystallography parameters were reported by Alonso¹⁷ and started with *Pbnm* and *P*₂₁/*n* space groups for the high- and low-temperature phases, respectively. The band structure and partial density of states (PDOS) of both structures are calculated.

Band structures of YNiO₃ show differences between the *Pbnm* and *P*₂₁/*n* phases (Figure 1). In the orthorhombic phase (Figure 1a), bands from –0.5 to +2 eV merge into one continuous band

* Corresponding author. Tel: 86-431-8499053. Fax: 86-431-8499061.
E-mail: jzhan@mail.jlu.edu.cn.

[†] Jilin University.

[‡] Beijing Institute of Technology.

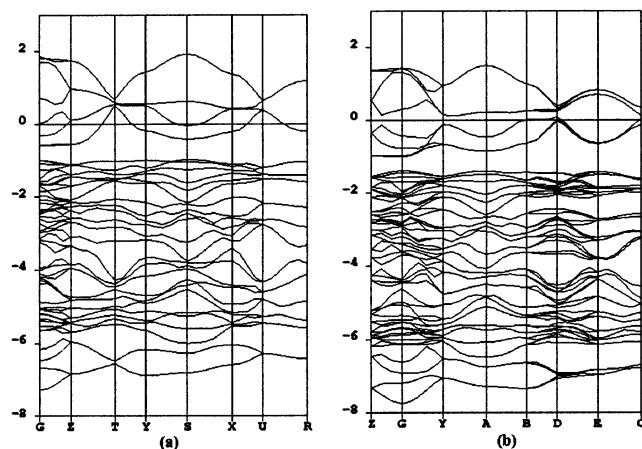


Figure 1. Band structures of YNiO_3 : (a) continuous band across the Fermi Level in the metallic orthorhombic phase; (b) gap opening at the Fermi level in the insulating monoclinic phase.

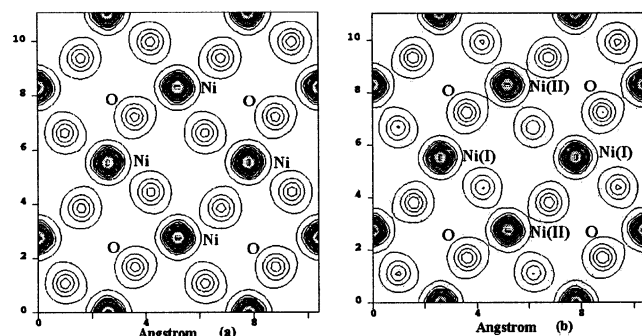


Figure 2. Electronic density maps of (001) plan of YNiO_3 : (a) same charge density of Ni ions in the metallic orthorhombic phase; (b) charge density of Ni(I) is different from that in Ni(II), indicating a charge disproportionation, in the insulating monoclinic phase.

across the Fermi level. The band structure exhibits a typical metallic characteristic, which shows that the orthorhombic phase is metallic. In the monoclinic phase, a gap opens with the minimum value at the k -point C (Figure 1b). Therefore, the band structure of $P2_1/n$ phase shows an insulating characteristic. It is worth noting the value of gap obtained within the density functional calculation. The normal error of the LDA in reproducing a gap in the wide-band systems is within 40%. The self-interaction error still increases if the involved orbitals become more localized. For a semiconductor, it has been shown computationally that most of the differences between Kohn–Sham eigenvalues and the true excitation energies can be explained by a rigid shift of the conduction bands upward with respect to the valence bands. It is hard to calculate a precise gap. However, whether there is a gap or not is very important to evaluate the conduction characteristic of the materials.

Electronic density maps presented in Figure 2 show the changes of charge distribution. It is clear that there is a homogeneous charge distribution for all the Ni ions in the orthorhombic YNiO_3 , as shown in Figure 2a. The charge density is different between Ni(I) and Ni(II) ions in the monoclinic YNiO_3 , as shown in Figure 2b, which reveals that there is a charge disproportionation between Ni(I) and Ni(II) ions. Calculation shows that there is a higher electron density in Ni(II) than in Ni(I).

The hybridization state of Ni-3d and O-2p can be investigated by PDOS. The PDOS of Ni-3d are presented in Figure 3. Ni(I) and Ni(II) represent two types of Ni ions in monoclinic phase. Ni represents Ni ions in orthorhombic phase. The band from

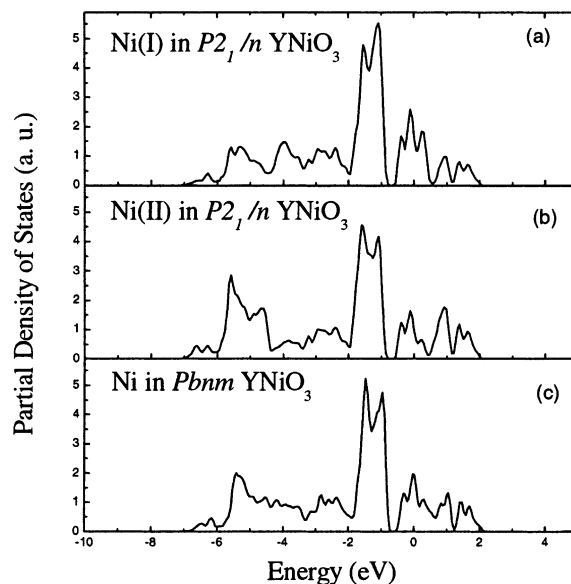


Figure 3. Calculated partial density of states of Ni-3d in YNiO_3 : (a) for Ni(I) ion in the insulating monoclinic phase; (b) for Ni(II) ion in the insulating monoclinic phase; (c) for Ni ion in the metallic orthorhombic phase.

TABLE 1: Integration Intensities of Ni-3d Bands in YNiO_3

atom	total	e_g^*	t_{2g}	e_g^b
Ni(I) ^a	9.86519	2.24656	3.85359	3.76503
Ni(II) ^a	9.80514	2.08917	3.37034	4.34562
Ni ^b	9.8398	2.17225	3.61287	4.05468

^a Ni in the monoclinic phase. ^b Ni in the orthorhombic phase.

−2 to −0.7 eV is denoted as the t_{2g} band, which inhabits mainly d_{xy} , d_{xz} , and d_{yz} orbitals point away from the oxygen and form nonbonding band. Bands from −7 to −2 eV are denoted as e_g^b band, which occupies the d_{z^2} and $d_{x^2-y^2}$ atomic orbitals directly overlapping with the p_x , p_y , and p_z orbitals of the oxygen along the octahedral directions.¹⁸ Calculation shows that for Ni(I), the integration intensities of the e_g^b and t_{2g} bands decrease and increase, respectively, compared to that of Ni. For Ni(II), the integration intensities of the e_g^b and t_{2g} bands increase and decrease, respectively, compared to that of Ni. The higher valence state of the Ni ion corresponds to a higher density of the e_g^b band, because the e_g^b band corresponds to the bonding state.¹⁸ Additionally, the t_{2g} band corresponds to the nonbonding state,¹⁸ so that the higher valence state corresponds to a lower density of the t_{2g} band. Thus it is concluded that Ni(I) and Ni(II) in the monoclinic $P2_1/n$ phase are in an inequivalent valence state, $\text{Ni}^{(3-\delta)+}$ and $\text{Ni}^{(3+\delta)+}$, respectively, according to the changes of the intensities of both e_g^b and t_{2g} bands in PDOS. There exists a single valence state Ni^{3+} in the orthorhombic phase.

The valence state of the Ni ions in both the orthorhombic and monoclinic phases can be obtained via the distribution of Ni-3d electrons in the t_{2g} and e_g^b bands. Integration of each band of Ni-3d PDOS is calculated and listed in Table 1. The antibonding e_g^* band consisting of the states from −0.7 to +2 eV is also included. The integration intensity of the bonding e_g^b band of Ni(I)-3d decreases 0.29 with respect to that of Ni in orthorhombic phase, which indicates 3d electrons participate in 3d–2p hybridization of Ni(I)–O less than those in Ni–O in the orthorhombic phase with an amount of 0.29. Correspondingly, an increasing of 0.24 in the integration intensity of the t_{2g} band of Ni(I) indicates that there are more localized

nonbonding Ni(I)-3d electrons. The discrepancy between changes of the integration intensities of the e_g^b and t_{2g} bands lies in the difference of covalent properties of Ni–O bonding concerned with charge transfer, which affects the integration of the e_g^b band. Therefore, the value of δ is calculated by the integration intensity of the t_{2g} band. The calculation indicates a decrease of 0.24 in the integration intensity of the t_{2g} band of Ni(II). As a result, the valence states of Ni(I) and Ni(II) are 2.76 and 3.24 in the monoclinic phase, respectively, based on the evidence that the valence state of Ni is 3 in *Pbmm* phase $YNiO_3$. In fact, δ reflects the changes of the Ni-3d electrons in the nonbonding t_{2g} band.

Acknowledgment. This work was supported by Chinese Natural Science Foundation, under Grant No. 50272023 and the Special Funds for Major State Basic Research Project of China under Grant No. 2002CB211802.

References and Notes

- (1) Lacorre, P.; Torrance, J. B.; Pannetier, J.; Nazzal, A. I.; Wang, P. W.; Huang, T. C. *J. Solid State Chem.* **1991**, *91*, 225–237.
- (2) Torrance, J. B.; Lacorre, P.; Nazzal, A. I.; Ansaldo, E. J.; Niedermayer, C. *Phys. Rev. B* **1992**, *45*, 8209–8212.
- (3) García-Muñoz, J. L.; Rodríguez-Carvajal, J.; Lacorre, P.; Torrance, J. B. *Phys. Rev. B* **1992**, *46*, 4414–4425.
- (4) Torrance, J. B.; Lacorre, P.; Asavaroengchai, C.; Metzger, R. M. *J. Solid State Chem.* **1991**, *90*, 168–172.
- (5) Medarde, M.; Fontaine, A.; García-Muñoz, J. L.; Rodríguez-Carvajal, J.; de Santis, M.; Sacchi, M.; Rossi, G.; Lacorre, P. *Phys. Rev. B* **1992**, *46*, 14975–14984.
- (6) Alonso, J. A.; Martínez-Lope, M. J.; Rasines, I. *J. Solid State Chem.* **1995**, *120*, 170–174.
- (7) Medarde, M. L. *J. Phys. Condens. Matter* **1997**, *9*, 1679–1707.
- (8) García-Muñoz, J. L.; Rodríguez-Carvajal, J.; Lacorre, P. *Phys. Rev. B* **1994**, *50*, 978–992.
- (9) García-Muñoz, J. L.; Rodríguez-Carvajal, J.; Lacorre, P. *Europhys. Lett.* **1992**, *20*, 241–247.
- (10) Demazeau, G.; Marbeuf, A.; Pouchard, M.; Hagenmuller, P. *J. Solid State Chem.* **1971**, *3*, 582–589.
- (11) Alonso, J. A.; García-Muñoz, J. L.; Fernández-Díaz, M. T.; Aranda, M. A. G.; Martínez-Lope, M. J.; Casais, M. T. *Phys. Rev. Lett.* **1999**, *82*, 3871–3874.
- (12) Alonso, J. A.; Martínez-Lope, M. J.; Casais, M. T.; Aranda, M. A. G.; Fernández-Díaz, M. T. *J. Am. Chem. Soc.* **1999**, *121*, 4754–4762.
- (13) Kim, S. J.; Demazeau, G.; Presniakov, I.; Pokholok, K.; Sobolev, A.; Ovanesyan, N. *J. Am. Chem. Soc.* **2001**, *123*, 8127–8128.
- (14) Brown, I. D. In *Structure and Bonding in Crystals*; O'Keeffe, M., Navrotsky, A., Eds.; Academic Press: New York, 1981; Vol. 2, pp 1–30.
- (15) Alonso, J. A.; Martínez-Lope, M. J.; Casais, M. T.; García-Muñoz, J. L.; Fernández-Díaz, M. T. *Phys. Rev. B* **2000**, *61*, 1756–1763.
- (16) Payne, M. C.; Teter, M. P.; Allan, D. C.; Arias, T. A.; Joannopoulos, J. D. *Rev. Mod. Phys.* **1992**, *64*, 1045–1097.
- (17) Alonso, J. A.; Martínez-Lope, M. J.; Casais, M. T.; García-Muñoz, J. L.; Fernández-Díaz, M. T.; Aranda, M. A. G. *Phys. Rev. B* **2001**, *64*, 094102.
- (18) Aydinol, M. K.; Kohan, A. F.; Ceder, G.; Cho, K.; Joannopoulos, J. *Phys. Rev. B* **1997**, *56*, 1354–1365.